Liao *et al. Journal of Translational Medicine* (2024) 22:715
https://doi.org/10.1186/s12967-024-05540-w

Journal of
Translational Medicine

RESEARCH

Open Access

# Suppression of NUPR1 in fibroblast-like synoviocytes reduces synovial fibrosis via the Smad3 pathway

Taiyang Liao[1,2], Lei Shi[1,2], Chenglong He[1,2], Deren Liu[1,2], Yibao Wei[1,2], Zhenyuan Ma[1,2], Peimin Wang[1], Jun Mao[1*] and Peng Wu[1*]

## Abstract

**Background** Synovial fibrosis is a common complication of knee osteoarthritis (KOA), a pathological process characterized by myofibroblast activation and excessive extracellular matrix (ECM) deposition. Fibroblast-like synoviocytes (FLSs) are implicated in KOA pathogenesis, contributing to synovial fibrosis through diverse mechanisms. Nuclear protein 1 (NUPR1) is a recently identified transcription factor with crucial roles in various fibrotic diseases. However, its molecular determinants in KOA synovial fibrosis remain unknown. This study aims to investigate the role of NUPR1 in KOA synovial fibrosis through in vivo and in vitro experiments.

**Methods** We examined NUPR1 expression in the murine synovium and determined the impact of NUPR1 on synovial fibrosis by knockdown models in the destabilization of the medial meniscus (DMM)-induced KOA mouse model. TGF-β was employed to induce fibrotic response and myofibroblast activation in mouse FLSs, and the role and molecular mechanisms in synovial fibrosis were evaluated under conditions of NUPR1 downexpression. Additionally, the pharmacological effect of NUPR1 inhibitor in synovial fibrosis was assessed using a surgically induced mouse KOA model.

**Results** We found that NUPR1 expression increased in the murine synovium after DMM surgical operation. The adeno-associated virus (AAV)-*NUPR1* shRNA promoted *NUPR1* deficiency, attenuating synovial fibrosis, inhibiting synovial hyperplasia, and significantly reducing the expression of pro-fibrotic molecules. Moreover, the lentivirus-mediated *NUPR1* deficiency alleviated synoviocyte proliferation and inhibited fibroblast to myofibroblast transition. It also decreased the expression of fibrosis markers α-SMA, COL1A1, CTGF, Vimentin and promoted the activation of the SMAD family member 3 (SMAD3) pathway. Importantly, trifluoperazine (TFP), a NUPR1 inhibitor, attenuated synovial fibrosis in DMM mice.

**Conclusions** These findings indicate that NUPR1 is an antifibrotic modulator in KOA, and its effect on anti-synovial fibrosis is partially mediated by SMAD3 signaling. This study reveals a promising target for developing novel antifibrotic treatment.

**Keywords** Knee osteoarthritis, Synovial fibrosis, Nuclear protein 1, Transforming growth factor beta, Smad family member 3

*Correspondence:
Jun Mao
maojun@njucm.edu.cn
Peng Wu
wupeng@njucm.edu.cn
Full list of author information is available at the end of the article

## Introduction

Knee osteoarthritis (KOA) is a progressive, degenerative joint disease that predominantly affects middle-aged and older individuals, accounting for a significant portion of global suffering, disability, and socioeconomic burden [1, 2]. Current research on KOA primarily focuses on articular cartilage degradation and subchondral bone sclerosis as its main phenotypic alterations. However, it overlooks that the synovium also exhibits considerable phenotypic changes, including tissue hyperplasia, immune cell and inflammatory mediator infiltration, prominent neoangiogenesis, and varying degrees of fibrosis [3]. The synovium is a delicate layer of connective tissue primarily consisting of fibroblast-like synoviocytes (FLSs) and tissue-resident macrophages, two distinct cell types with vital roles in joint physiology. It synthesizes synovial fluid, an essential medium that sustains articular chondrocytes and facilitates the clearance of metabolic by-products [4]. Fibroblast-like synoviocytes are pivotal cells in synovial fibrosis and respond to pro-inflammatory stimuli by secreting collagen, causing the gradual build-up of the extracellular matrix (ECM) [5]. This process precipitates synovial hyperproliferation, hypertrophy, and extensive fibrosis, provoking the clinical manifestations of joint stiffness and pain [5]. Clinically, synovial fibrosis is a principal etiological factor that limits joint mobility and impacts approximately half of the individuals diagnosed with osteoarthritis [6]. Therefore, understanding the intricate regulatory network controlling synovial fibrosis in KOA is crucial for devising effective treatments for patients with this disease.

In KOA-related synovial fibrosis, phenotypic changes in FLSs occur primarily due to their differentiation into myofibroblasts, triggering the overproduction and secretion of ECM components, especially collagen type I alpha 1 (COL1A1) [7, 8]. The fibroblast to myofibroblast transition is characterized by elevated α-smooth muscle actin (α-SMA) expression and heightened proliferative capacity [9]. Myofibroblasts exhibit increased expression of mesenchymal markers such as COL1A1, Vimentin, connective tissue growth factor (CTGF), and α-SMA [10]. Transforming growth factor β1 (TGF-β1) plays a crucial role in the fibrosis of various tissues, such as the kidneys, liver, and heart, regulating cell proliferation, differentiation, immunity, and wound healing. Its underlying mechanisms in fibrosis primarily involve the activation of the TGF-β1/SMAD family member 3 (TGF-β1/SMAD3) signaling pathway [11]. This signaling pathway has been extensively studied in the synovial fibrosis research field and is considered a critical mechanism in KOA development [12–14]. Synoviocytes release high concentrations of TGF-β into the synovial fluid of patients with KOA [15]. By injecting 50 ng of TGF-β, it is possible to increase the number of cells in the synovial lining by stimulating synoviocyte proliferation and collagen deposition [16]. Moreover, directly injecting TGF-β into a mouse knee joint promotes synovial hyperplasia and contributes to osteophyte formation [17]. The physiological functions of the SMAD3 protein depend on its phosphorylation level and intracellular localization. When cells are stimulated by inflammation or undergo a fibrotic response, SMAD3 is phosphorylated and translocated to the nucleus, regulating the expression of α-SMA, COL1A1, Vimentin, and many other genes [16, 18]. Thus, blocking the SMAD3 signaling pathway could be an effective strategy against KOA synovial fibrosis.

Nuclear protein 1 (NUPR1) is a transcription factor whose activation has been discovered as a response to pancreatitis-induced cellular damage [19]. Typically, it is expressed at high levels in response to stress, such as inflammatory stimulation, endoplasmic reticulum stress, oxidative stress injury, and amino acid deprivation, indicating the host microenvironment expression determines NUPR1 expression [20].

Functionally, NUPR1 is involved in numerous cellular processes, such as cell cycle progression, oxidative stress management, apoptosis initiation, onset of senescence, autophagy activation, and facilitation of DNA repair mechanisms [21–24]. Hence, it has a role in the development of various diseases, with research primarily focusing on different types of cancer, such as liver, oral, and bladder cancers [25–27]. Moreover, NUPR1 contributes to KOA progression based on recent evidence: (1) NUPR1 levels increase in human KOA cartilage as well as in cartilage from older monkeys treated with DMM [28, 29]; (2) NUPR1 is highly expressed in chondrocytes under tert-butyl hydrogen peroxide-triggered stress, and matrix metallopeptidase 13 (MMP13) is induced by stress and inflammation [28]; and (3) Induction of NUPR1 and tribbles pseudokinase 3 (TRB3) expression regulates chondrocyte apoptosis [30]. Although the role of NUPR1 in renal and pancreatic fibrosis has been recently established [31, 32], little is known about its involvement in KOA and synovial fibrosis.

In this study, we found that NUPR1 expression increased in mouse synovium after surgical DMM, and suppressing NUPR1 expression mitigated DMM-induced synovial fibrosis. Mechanistically, NUPR1 deficiency alleviated TGF-β-induced synovial fibrosis and reversed the TGF-β-induced myofibroblast activation by promoting the activation of SMAD3 signaling. Remarkably, pharmacologic NUPR1 inhibition using trifluoperazine (TFP) reduced synovial fibrosis in DMM-operated mice.

## Results

### NUPR1 is upregulated in the synovium of the osteoarthritis mouse model

We performed destabilization of medial meniscus (DMM) operation on C57BL/6J mice (20–22 g) to confirm the effectiveness of the knee osteoarthritis model (Fig. 1A). We evaluated the condition of the knee joint (red box in Fig. 1B) with X-ray imaging at 8 weeks postoperatively. We uncovered that the KOA group had severely narrowed joint space, uneven knee joint surface, significant cartilage defects, and marginal osteophyte formation versus the sham group, confirming obvious signs of knee osteoarthritis. Moreover, Kellgren-Lawrence grading indicated a grade of 0 in the sham group and a grade of 2 to 3 in the KOA group (Fig. S1A). In addition, we performed hematoxylin and eosin (HE), Masson, and Sirius red staining to assess the pathological changes of the synovium in the model. We observed severe synovial pathologic changes in the DMM-induced KOA model, including synovitis with a high score,

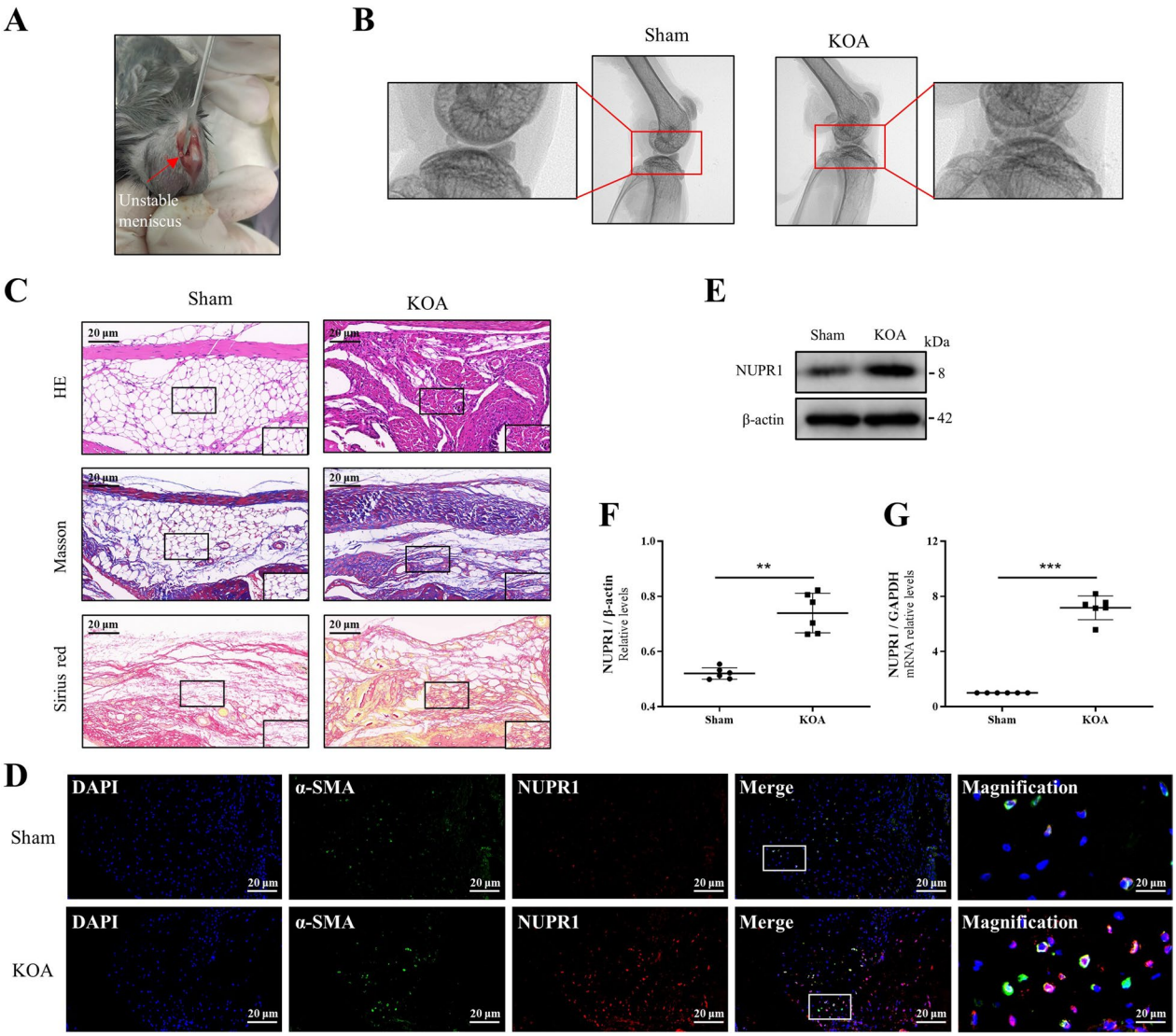


**Fig. 1** Nuclear protein 1 (NUPR1) is upregulated in the synovium of the osteoarthritis mouse model. **A** Destabilization of medial meniscus (DMM) surgical procedure was performed in C57BL/6J mice (20–22 g). **B** Representative X-ray images were obtained in C57BL/6J mice 8 weeks after surgical DMM ($n=6$ mice per group). **C** Representative images showing HE, Masson, and Sirius red staining at ×400 magnification ($n=6$ mice per group). Scale bar, 20 μm. **D** Representative co images of NURP1 and α-SMA protein in the synovium of DMM- or sham-operated mice detected by immunofluorescence staining at ×400 magnification ($n=6$ mice per group). Scale bar, 20 μm. **E**, **F** Immunoblotting analysis of NUPR1 expression in synovial tissues of DMM- or sham-operated mice ($n=6$ mice per group). **G** The relative expression of *NUPR1* mRNA quantified with RT-qPCR in synovial tissues of DMM- or sham-operated mice ($n=6$ mice per group). $^{**}P<0.01$, $^{***}P<0.001$ calculated by unpaired 2-tailed *t* test

aberrant collagen I deposition, and increased area of synovial fibrosis (Fig. 1C and S1B-D). Finally, we compared NUPR1 expression at the protein and mRNA level in the synovium of the sham and KOA groups with immunofluorescence, Western blotting, and RT-qPCR. We demonstrated that NUPR1 expression in fibrotic synovial tissues of the KOA group was enhanced compared with that of the sham group (Fig. 1D–G). These results indicate that NUPR1 expression is upregulated in the synovium of mice with DMM-induced KOA.

### NUPR1 deficiency attenuates synovial fibrosis in the KOA mouse model

Male 10-week-old C57BL/6J mice were given an intra-articular injection of adeno-associated virus (AAV) expressing *NUPR1*-specific shRNA (hereafter *AAV-shNUPR1*) to determine whether *NUPR1* plays a role in synovial fibrosis (Fig. 2A). The efficiency of *AAV-shNUPR1* in the joints was verified by western blotting and RT-qPCR (Fig. 2B and S2A, B). Next, we performed a sequence of experiments to determine whether *AAV-shNUPR1* reduces the degree of synovial fibrosis in the KOA mouse model. On days 28, 42, and 56 after the operation, the degree of swelling in the knee joints was measured by vernier calipers. While the mice in the DMM + *AAV-shNC* group exhibited significant swelling in the knee joints, those treated with *AAV-shNUPR1* showed alleviated swelling (Fig. 2C). Subsequently, Masson staining of the knee was performed 8 weeks after DMM to assess the severity of synovial fibrosis (Fig. 2D). It revealed that mice in the DMM + *AAV-shNC* group had a higher percentage of the blue fibrotic area than those in the Sham + *AAV-shNC* group, suggesting the mice who underwent DMM had severe synovial fibrosis. Remarkably, mice injected with *AAV-shNUPR1* showed reduced synovial fibrosis after DMM compared with those injected with control shRNA (Fig. 2E). Western blotting and RT-qPCR also revealed increased expression of 4 crucial synovial fibrosis markers: *α-SMA*, *COL1A1, CTGF*, *Vimentin,* and this effect was attenuated upon *NUPR1* knockdown (Fig. 2F–J and S2C–F). In summary, these findings suggest that NUPR1 deficiency relieves synovial fibrosis in the DMM-induced KOA model.

### NUPR1 deficiency inhibits synovial hyperplasia and synoviocyte proliferation

Next, we stained knee joint tissue with hematoxylin and eosin (HE) to assess synovial hyperplasia [33]. The synovial thickness of mice in the DMM + *AAV-shNC* group was considerably higher than that of mice in the Sham + *AAV-shNC*. Remarkably, the synovial thickness in the DMM + *AAV-shNUPR1* group was dramatically reduced compared with the DMM + *AAV-shNC* group (Fig. 3A, B). In the pathological process of KOA, excessive synoviocyte proliferation is one of the chief causes of synovial fibrosis [10, 34]. Fibroblast-like synoviocytes (FLSs) were isolated from the synovium of the knee joint, and cell proliferation was induced by TGF-β [35]. The expression levels of NUPR1 protein and mRNA, along with the fibrosis markers α-SMA and COL1A1, were evaluated in TGF-β-stimulated FLSs. It was observed that the expression of these three genes—NUPR1, α-SMA, and COL1A1—increasingly enhanced with time of TGF-β intervention (0–24 h) (Fig. S3A-G). Next, we transduced FLSs with a lentivirus expressing control (*shCtrl*) or *NUPR1* shRNA (*shNUPR1*) to investigate the role of *NUPR1* in TGF-β-induced synoviocyte proliferation. After TGF-β stimulation, more EdU-positive cells (indicated by red fluorescence) were observed among *shNUPR1*-transduced FLSs than among the *shCtrl*-transduced. Conversely, a significant decrease in EdU-positive cells was found among *shNUPR1*-transduced FLSs versus the *shCtrl*-transduced FLSs following TGF-β + *shNUPR1* treatment (Fig. 3C, D). These data suggest that NUPR1 deficiency inhibits synovial hyperplasia and limits FLS cell proliferation.

### NUPR1 is essential for TGF-β-induced fibrotic response in FLSs by promoting SMAD3 signaling

Evidence indicates that NUPR1 and SMAD3 signaling mediates the expression of fibrotic markers α-SMA, COL1A1, and Vimentin [31, 32]. Therefore, we hypothesized that NUPR1 regulates the expression of these genes

(See figure on next page.)

**Fig. 2** NUPR1 deficiency attenuates synovial fibrosis in the KOA mouse model. **A** Timeline of animal experiment. **B** The effectiveness of adeno-associated virus (AAV) carrying *NUPR1*-specific shRNA (*AAV-shNUPR1*) was determined by RT-qPCR. Synovium was obtained 10 weeks after intra-articular injection of *AAV-shNC* (AVV bearing scramble shRNA) or *AAV-shNUPR1* ($n = 6$ mice per group). **C** Vernier calipers were used to measure the degree of swelling in mouse knee joints on days 28, 42, and 56 following DMM surgical intervention ($n = 6$ mice per group). **D** Representative Masson staining images of mouse knee joints at ×200 magnification ($n = 6$ mice per group). Scale bar, 50 μm. Two weeks before surgery, male 10-week-old C57/BL6J mice were injected intra-articularly with *AAV-shNUPR1* and analyzed 8 weeks after surgery. **E** Quantification of the percentage of fibrotic area (%) of mouse synovial tissue ($n = 6$ mice per group). **F–J** Immunoblotting analysis of α-SMA, COL1A1, CTGF, and Vimentin protein expression in synovial tissues ($n = 6$ mice per group). $^{**}P < 0.01$, $^{***}P < 0.001$. Unpaired 2-tailed *t* test (**B**); 1-way ANOVA (**C**–**I**)

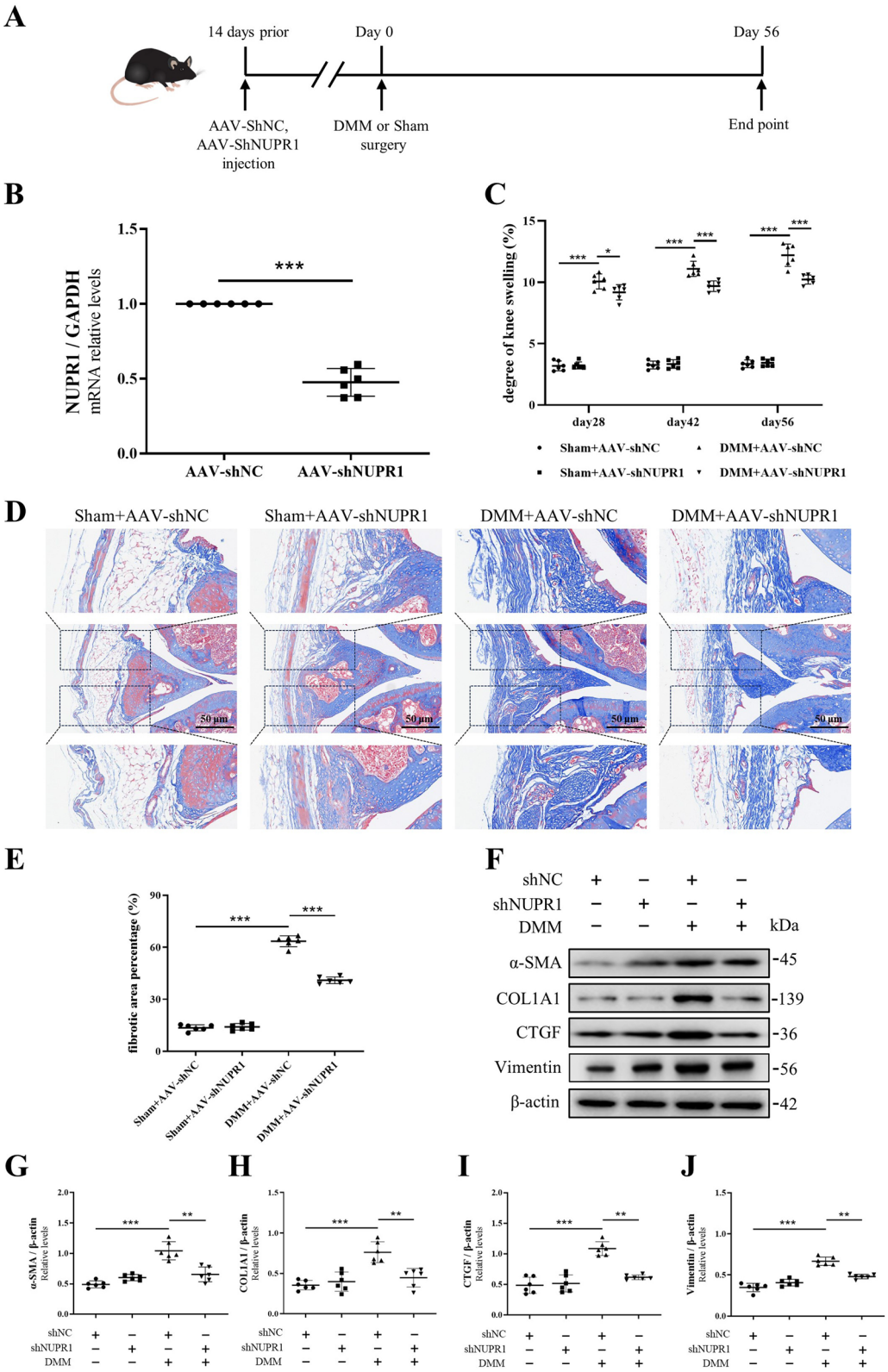


**Fig. 2** (See legend on previous page.)

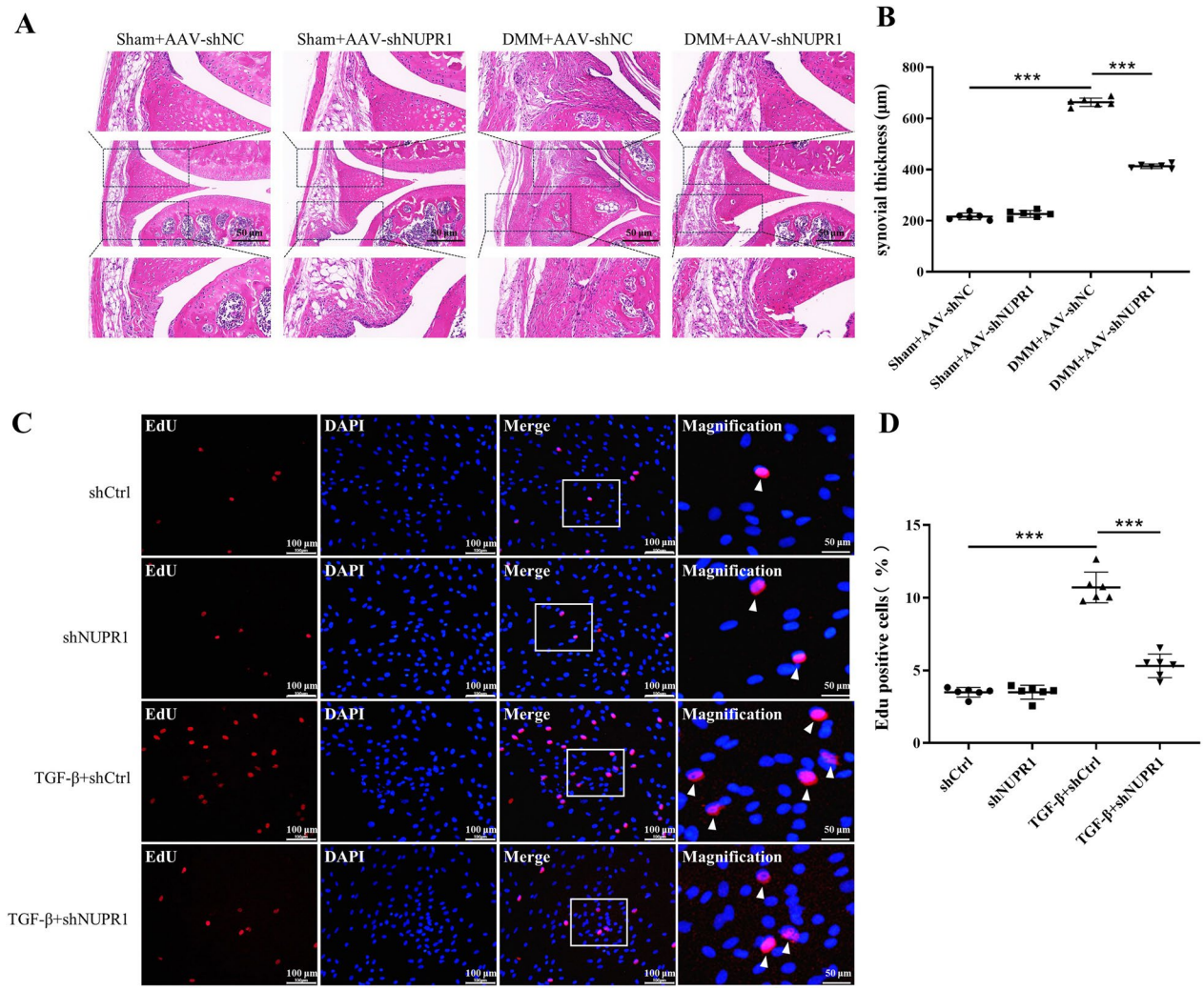


**Fig. 3** NUPR1 deficiency inhibits synovial hyperplasia and synoviocyte proliferation. **A** Representative images showing HE staining of the synovium of mouse knee joints at ×200 magnification ($n=6$ mice per group). Scale bar, 50 μm. **B** Synovial hyperplasia was assessed by measuring synovial thickness ($n=6$ mice per group). **C** FLSs were transduced with a lentivirus carrying *shNC* (scramble shRNA) or *shNUPR1* (*NUPR1* shRNA) followed by vehicle (–) TGF-β treatment for 24 h, as indicated. Representative images of EdU staining of FLSs at ×200 or ×400 magnification ($n=6$ mice per group). EdU-positive cells are depicted in red, while DAPI-stained nuclei are in blue. Scale bar, 100 μm or 50 μm. **D** Quantification of EdU-positive cells ($n=6$ mice per group). ***$P<0.001$. 1-way ANOVA (**A**–**D**)

through the SMAD3 signaling pathway. To evaluate our hypothesis, we used a lentiviral vector containing *shCtrl* (scramble shRNA) or *NUPR1* shRNA (*shNUPR1*) to infect FLSs and stimulate them with TGF-β. We quantified *NUPR1* mRNA expression in FLSs, uncovering it was upregulated in the TGF-β + *shCtrl* group but downregulated after *NUPR1* knockdown (Fig. 4A). Subsequently, we examined the expression of the α-SMA protein, a myofibroblast marker, using immunofluorescence staining. The results indicated that the expression of α-SMA was reduced when FLSs were transduced with *shNUPR1* and subsequently exposed to TGF-β stimulation (Fig. 4B, C). Moreover, consistent with our observation in the synovium of *NUPR1* knockdown KOA mice, *shNUPR1*-transduced synoviocytes exhibited reduced TGF-β-induced fibrosis that was also reflected in decreased *α-SMA*, *COL1A1*, *CTGF* and *Vimentin* protein levels. Thus, the results demonstrate that *NUPR1* knockdown significantly blocks TGF-β-induced *α-SMA*, *COL1A1*, *CTGF* and *Vimentin* expression (Fig. 4D–H and S4A–D). Furthermore, TGF-β-induced SMAD3 phosphorylation in FLSs was inhibited following *NUPR1* knockdown (Fig. 4I, J), indicating that NUPR1 regulates *α-SMA*, *COL1A1*, *CTGF* and *Vimentin* expression via SMAD3 signaling. Since a 30-min TGF-β treatment induces SMAD3 nuclear translocation [16], we investigated

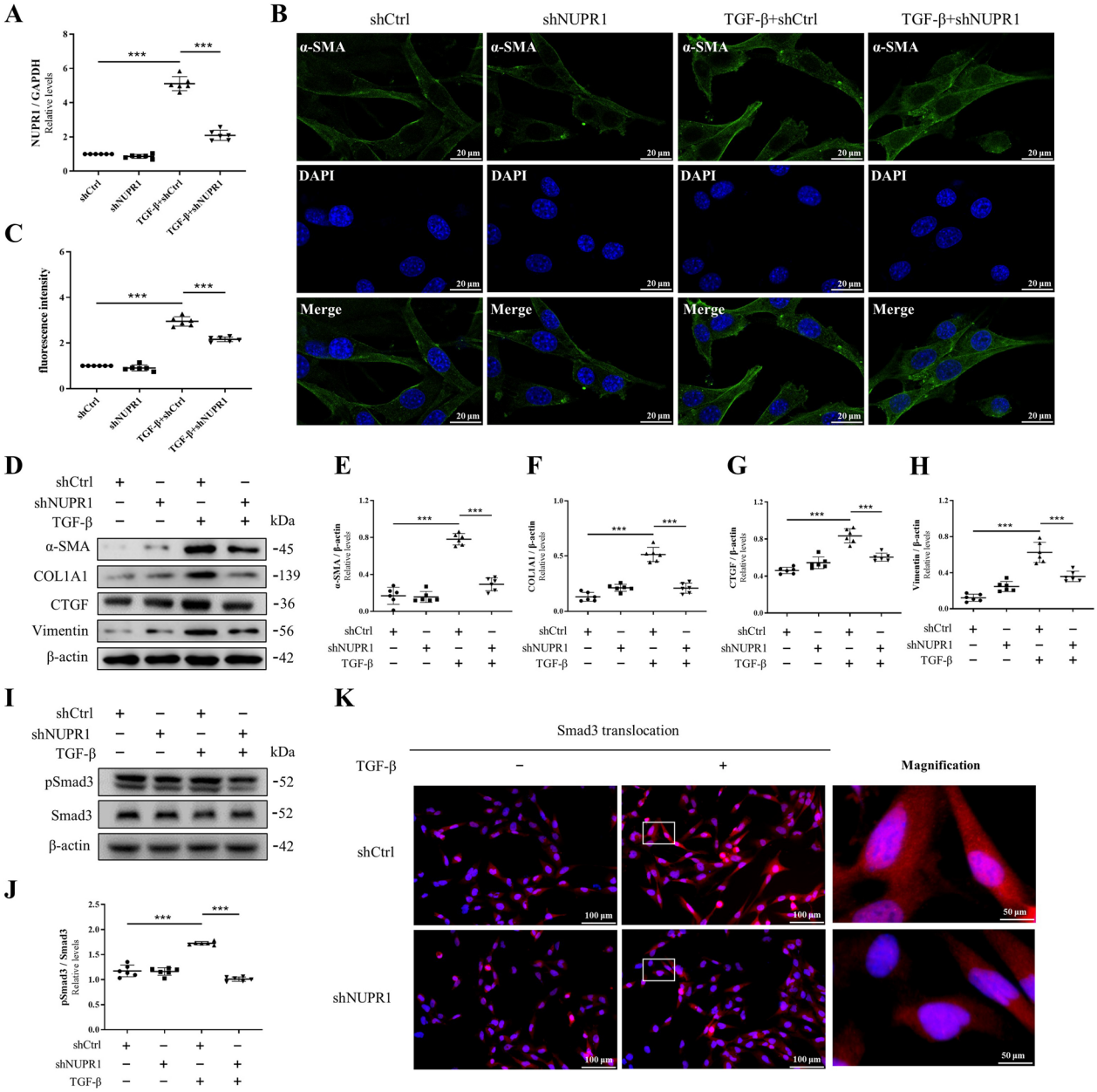


**Fig. 4** NUPR1 is essential for TGF-β-induced fibrotic response in FLSs by promoting SMAD3 signaling. **A** FLSs were stimulated with 50 ng/mL TGF-β for 24 h. Relative expression of *NUPR1* in FLSs ($n=6$ mice per group) quantified with RT-qPCR. **B** FLSs were stimulated with 50 ng/mL TGF-β for 24 h. Representative immunofluorescence staining images of α-SMA (green) in FLSs at ×630 magnification ($n=6$ mice per group). Scale bar, 100 μm. **C** Quantification of fluorescence intensity ($n=6$ mice per group). **D–J** FLSs were stimulated with 50 ng/mL TGF-β for 24 h. Immunoblotting analysis of α-SMA, COL1A1, CTGF, Vimentin, pSmad3, and Smad3 protein expression in FLSs ($n=6$ mice per group). **K** FLSs were stimulated with 50 ng/mL TGF-β for 0.5 h. Representative immunofluorescence staining of SMAD3 cellular location (red) in the FLSs at ×200 or ×400 magnification ($n=6$ mice per group). Scale bar, 100 μm or 50 μm. ***$P<0.001$. 1-way ANOVA (**A**–**J**)

whether NUPR1 contributes to SMAD3 nuclear localization by immunofluorescence staining. When FLSs were exposed to a 30-min TGF-β activation, the SMAD3 protein translocated to the FLS nuclei. However, FLSs treated with TGF-β+*shNUPR1* showed significantly reduced SMAD3 nuclear localization compared with cells treated with TGF-β+*shCtrl* (Fig. 4K). These data imply that silencing *NUPR1* not only reverses the TGF-β-induced fibroblast differentiation into myofibroblasts and lowers α-SMA expression but also mitigates TGF-β-induced

synovial fibrosis by inhibiting SMAD3 phosphorylation and affecting SMAD3 nuclear localization in FLSs.

### Trifluoperazine (TFP) reduces synovial fibrosis in DMM-induced mouse KOA

Trifluoperazine (TFP) is a robust calmodulin inhibitor that effectively targets central dopamine receptors and is an FDA-approved conventional antipsychotic used to relieve anxiety. It also binds NUPR1 and prevents it from associating with other proteins, abrogating NUPR1 function and mimicking the effects of NUPR1 deficiency [36, 37]. TFP administration presents a substantial therapeutic prospect in ameliorating fibrotic disorders since it hinders apoptosis and inflammatory cascades, attenuating fibrotic progression in cardiac and renal tissues [37, 38]. Because our investigation revealed that NUPR1 is indispensable in synovial fibrosis pathogenesis, we investigated whether TFP-induced NUPR1 inactivation ameliorates the pathological alterations induced by DMM. As expected, whereas collagen deposition significantly increased in DMM-operated mice, TFP treatment significantly decreased collagen deposition (Fig. 5A, B). Moreover, TFP treatment significantly lessened synovial hyperplasia, as evidenced by HE staining quantification of synovial thickness (Fig. 5C, D). Western blotting and RT-qPCR quantification also revealed enhanced expression of *α-SMA*, *COL1A1*, *CTGF* and *Vimentin* after DMM operation, and this effect was further attenuated by TFP treatment (Fig. 5E–I and S5A–D). Further investigation is required to delineate the molecular pathways implicated in the TFP-induced NUPR1 downregulation. In conclusion, these findings indicate that pharmacologic NUPR1 inhibition reduces synovial fibrosis, potentially establishing NUPR1 as a viable therapeutic target for clinical trials.

## Materials and methods

### Experimental KOA model

Wildtype 10-week-old male C57BL/6J mice (20–22 g) were purchased from the Nanjing University of Chinese Medicine Laboratory Animal Center and bred in strict accordance with laboratory animal feeding guidelines. The experimental KOA model was induced in mice by surgical destabilization of the medial meniscus (DMM) that involves dissecting the medial meniscus ligament of the right knee [39]. Mice in the Sham group underwent a similar surgical procedure but without the medial meniscus ligament dissection. Mice were randomly assigned into 4 groups: Sham + *AAV-shNC*, Sham + *AAV-shNUPR1*, DMM + *AAV-shNC*, and DMM + *AAV-shNUPR1*. Mice were randomly allocated into 3 groups before trifluoperazine (TFP) administration: Sham, DMM, and DMM + TFP. Vehicle solution or 1.5 mg/kg TFP (MedChemExpress, USA) was intraperitoneally injected into mice with DMM for 3 days [31]. The mice were euthanized 7 days following DMM.

All experimental procedures were ethically approved by the Institutional Animal Care and Use Committee of Nanjing University of Chinese Medicine (ethics registration No. 202302A016) and performed following the governmental recommendations for the Care and Use of Laboratory Animals. All efforts to minimize pain and distress in C57BL/6 J mice were used.

### Adeno-associated virus (AAV) shRNA production and injection

For knockdown experiments, constructs *AAV-shNC* (Hanbio Biotechnology Co., Ltd, China) and *AAV-shNUPR1* (Hanbio) were used. A scramble (negative control, NC) or *NUPR1*-targeting shRNA sequence was subcloned into the *pHBAAV-U6-MCS-CMV-EGFP* vector (AAV serotype 5, AAV5) by Hanbio (shRNA sequences are shown in Supplementary Table S1). The *pHBAAV-shNUPR1-CMV-EGFP*, *pHelper*, and *pAAV-RC* vectors were co-transfected into AAV-293 cells using LipoFiterTM transfection reagent (Hanbio) to generate the recombinant adeno-associated virus. Before injecting AAV into the knee joint cavity, mice were anesthetized with 0.5% pentobarbital, and the skin over the joint area was shaved. Mice were injected intra-articularly with 10 μL of $1 \times 10^{10}$ vg/mL *AAV-shNC* or *AAV-shNUPR1* using 0.26-mm gauge needles and 10 μL microliter syringes (Shanghai Bolige Industry & Trade Co., Ltd., China) 14 days before DMM. The doses of AAV joint injections were chosen as reported previously [39, 40]. After treatment administration, the mice were placed on a 37 °C temperature-controlled surface and monitored until they regained consciousness and recovered. After a 56-day treatment period, euthanasia was performed on all mice by inhaling a lethal dose of $CO_2$, and the knee joints were harvested following the respective experimental protocols.

### Measurement of knee joint swelling

The degree of swelling was quantified on the day of modeling and 28, 42, and 56 days after the surgical procedure. The transverse diameter (mm) of the right knee joint within each group was measured by vernier calipers (Mitutoyo Corporation). The swelling percentage of the knee was computed using the formula: Knee Swelling (%) = ([Diameter of Right Knee Joint − Diameter of Left Knee Joint]/Diameter of Left Knee Joint) × 100.

### Histological analysis

Synovial or knee joint tissue sections were deparaffinized and hydrated with gradient alcohol, stained with

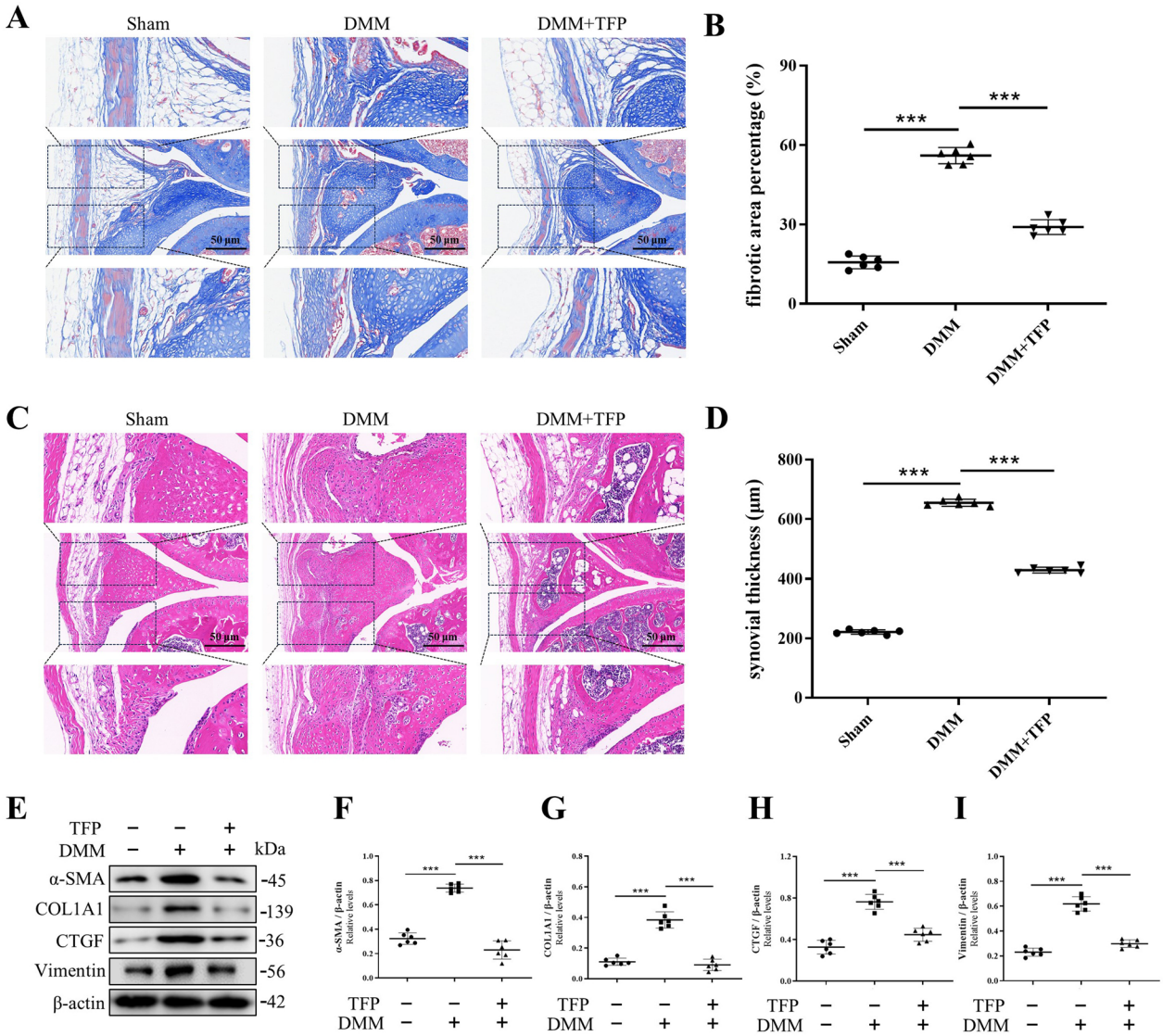


**Fig. 5** Trifluoperazine (TFP) reduces synovial fibrosis in DMM-operated mice. **A** Representative Masson staining images of mouse knee joints at ×200 magnification ($n = 6$ mice per group). Scale bar, 50 μm. Mice that underwent DMM received intraperitoneal injections of 1.5 mg/kg TFP for 3 days and were euthanized 7 days following DMM. **B** Quantification of the percentage of fibrotic area (%) in mouse synovial tissue ($n = 6$ mice per group). **C** Representative HE staining images of the synovium from mouse knee joints at ×200 magnification ($n = 6$ mice per group). Scale bar, 50 μm. **D** Synovial hyperplasia was assessed by measuring synovial thickness ($n = 6$ mice per group). **E–I** Immunoblotting analysis of α-SMA, COL1A1, CTGF, and Vimentin protein expression in synovial tissues ($n = 6$ mice per group). ***$P < 0.001$. 1-way ANOVA (**A**–**H**)

hematoxylin and eosin (HE) (Solarbio, China) or Masson's trichrome solution (Solarbio), dehydrated with gradient alcohol, and sealed with neutral gum. Subsequent histopathologic changes were monitored and recorded using an optical microscope (PerkinElmer Vectra 3.0). Each synovial tissue sample was prepared as 10 sequential HE-stained sections, and these were used to identify the thickest part of the synovium for thickness evaluation. These measurements were done using the Fiji software (ImageJ v. 1.74, NIH, USA; http://rsbweb.nih.gov/ij/). Synovial hyperplasia was determined by 2 blinded observers to assess pathological alterations in the synovial tissue [10]. Semiquantitative evaluation of synovitis was done using the Krenn scoring system with a 0 to 9 range [41]. The degree of synovial fibrosis was assessed by calculating the fibrotic area percentage (%) and the collagen I-positive areas (%) with the Fiji software.

#### Fibroblast-like synoviocyte (FLSs) isolation and culture

Knee-derived primary FLSs were isolated from the synovium of C57BL/6J mice (aged 8–12 weeks) by enzymatic digestion, as reported previously [42]. In brief, the synovium was removed from the anterior, medial, and lateral parts of the knee and the fat pad [43]. It was diced into 1-$mm^3$ fragments, enzymatically digested using 0.2% collagenase I (Solarbio) for 1 h while agitating at 500 rpm at 37 °C and vortexing at 20-min intervals. Subsequently, it was centrifuged at the appropriate speed, and the FLSs pellet was resuspended in DMEM (Biochannel, China) supplemented with 10% fetal bovine serum (FBS) (Biochannel), and 1×antibiotic–antimycotic (Solarbio). To preserve the FLS phenotype, cells were passaged when the primary FLS cultures attained approximately 80% confluence. For consecutive experiments, FLSs from 3d to 5th passage were selected. A portion of the extracted FLSs were cryopreserved in liquid nitrogen using serum-free cell cryopreservation solution (Cellregen Life Science and Technology Co., Ltd., China) for subsequent experimental use.

#### Lentiviral shRNA transduction

The mouse *NUPR1* shRNA (Hanbio) or scramble shRNA (negative control, shCtrl, Hanbio) was synthesized and inserted into the lentiviral vector *pHBLV-U6-MCS-CMV-ZsGreen-PGK-PURO* (Hanbio). Packaging vector *pSPAX2*, envelope vector *pMD2.G*, and *pHBLV-U6-shNUPR1-CMV-ZsGreen-PGK-PURO* were co-transfected into HEK293 cells using LipoFiterTM transfection reagent (Hanbio) to generate an infectious lentiviral particle. For lentiviral transduction, FLSs were seeded onto 6-well plates at a seeding density of $2\times10^5$ cells per well for 24 h and transduced with lentivirus-carrying shRNA constructs to establish a stable *NUPR1* downregulation (shRNA sequences are listed in Supplementary Table S2). Cells were exposed to the lentivirus at a $1\times10^8$ TU/mL titer in the presence of 10 μg/mL polybrene (Hanbio) following the manufacturer's instructions [44]. The validation of the mouse *NUPR1* downregulation vector was confirmed with sequencing analysis. After infection, FLSs were stimulated with 50 ng/mL TGF-β (MedChemExpress) for 0.5 or 24 h under serum-starved (0.5% FBS) medium conditions [16].

#### 5-Ethynyl-2′-deoxyuridine proliferation assay

Synoviocyte proliferation was assessed by 5-ethynyl-2′-deoxyuridine (EdU) staining performed with the Beyo-Click EdU Cell Proliferation Kit with Alexa Fluor 594 (Beyotime, China). Fibroblast-like synoviocytes were washed 3×with PBS, followed by adding a sequence of reagents: fresh DMEM with 10 μM EdU working solution, 4% paraformaldehyde, 0.3% Triton X-100, Click reaction solution, and DAPI (Absin). The incubation time in each reagent was done following the manufacturer's instructions. Cells were washed in PBS and observed under an inverted fluorescence microscope (#D3000, Leica, Germany).

#### Immunofluorescence staining

Immunofluorescence (IF) staining of mouse synovial tissues or FLSs was performed as described previously [45]. Tissues or cell slides were incubated overnight with primary antibodies: anti-NUPR1 (Bioss, China), anti-α-SMA (Abcam, USA) or anti-SMAD3 (Abcam). An incubation with corresponding CoraLite594- or Fluor488-conjugated secondary antibodies was done at 4 °C, followed by labeling the nuclei with DAPI (Absin) for 10 min. Images of target proteins were visualized and captured by an inverted fluorescence microscope (#D3000, Leica) or a Confocal Laser Scanning Microscope (#FV3000, Olympus). Quantification of IF staining results was performed using ImageJ software.

#### Western blotting

An appropriate amount of synovial tissue or FLSs was added to a RIPA Lysis Buffer (APExBIO, USA) containing phosphatase and proteinase inhibitors (10×V) (New Cell & Molecular Biotech Co., Ltd., China), followed by homogenization, ice-cold lysis, and centrifugation at 4 °C and 12,000 rpm from 5 to 10 min. The supernatant was collected, and the protein concentration was determined using a Pierce BCA Protein Assay Kit (Thermo Fisher Scientific Inc., USA). Next, proteins were separated on an SDS-PAGE gel (sodium dodecyl sulfate–polyacrylamide gel electrophoresis) (Vazyme Biotech Co., Ltd., China) and transferred onto polyvinylidene fluoride membranes (Merck, USA). The membranes were blocked for 1 h in 10 mM Tris-buffered saline (TBS) (Beyotime) containing 5% skimmed milk powder (Beyotime). They were probed for 12 h at 4 °C with one of the following antibodies diluted in 5% milk-TBS blocking buffer: anti-NUPR1 (Bioss), anti-α-SMA (Abcam), SMAD3 Antibody (Cell Signaling Technology), anti-phospho-SMAD3 (HUABIO), anti-COL1A1 (Proteintech Group, Inc.), anti-CTGF (Signalway Antibody LLC.), anti-Vimentin (ZEN-BIOSCIENCE, China), or anti-β-actin (Signalway Antibody LLC., USA). Membranes were washed 3×in TBS containing 0.1% Tween 20 and incubated for 1 h at room temperature with HRP conjugated secondary antibodies diluted in 5% milk-TBS blocking buffer: anti-rabbit (40 ng/mL; Sigma-Aldrich, Germany) and anti-mouse (1:10,000; Sigma-Aldrich). After multiple washes with Tween 20, membranes were treated with an ECL chemiluminescence substrate (Keygen BioTECH, China), and protein bands were visualized using an ImageQuant

imaging system (#800, GE HealthCare). Band signal intensity was quantified by normalizing the bands of interest to β-actin using Image Lab software (#6.1, Bio-Rad Laboratories, Inc.). Detailed information about the antibodies is presented in Supplementary Table S3.

#### Reverse transcription-quantitative PCR (RT-qPCR)

Total RNA was extracted from cellular and tissue samples using TRIzol reagent (Yeasen Biotechnology Co., Ltd., China), adhering to the manufacturer's protocol. Total RNA concentration and purity were assessed. Subsequently, total RNA was reverse transcribed into cDNA using the Hifair III 1st Strand cDNA Synthesis Kit (Yeasen). The cDNA was subjected to quantification with the Hieff qPCR SYBR Green Master Mix (Yeasen) in an ABI-7500 detection system (Applied Biosystems). The relative expression of each gene was normalized using the *Gapdh* gene as an internal reference and calculated with the $2^{-\Delta\Delta Ct}$ method (see Supplementary Table S4 for primer sequences). All primers were procured by Generay.

#### Statistical analysis

Statistical analyses were performed using GraphPad Prism 9.0 (GraphPad Software, Inc., La Jolla, CA, USA), and data were presented as means ± standard deviation. When 2 groups were compared, an unpaired 2-tailed *t* test was used. More than 2 groups were evaluated with a 1-way analysis of variance (ANOVA). Tukey's post-test was performed to compare differences between groups. A difference was significant when *P* values were $^{*}P < 0.05$, $^{**}P < 0.01$, and $^{***}P < 0.001$.

## Discussion

Knee osteoarthritis (KOA) is the most common chronic degenerative disease in the middle-aged and older population [1]. Synovial fibrosis usually occurs in the late stages of KOA progression and is characterized by progressive deterioration of the surrounding soft tissue, especially synovial tissue, as articular cartilage degeneration worsens. Consequently, joint pain, swelling, stiffness, functional impairments, and even disability arise [3]. Accumulating evidence shows that synovial fibrosis is highly associated with joint swelling, pain, and impaired motion [5, 6], demanding investigation of its specific pathological mechanism.

Human genes, such as *COL1A1*, *CTGF*, *Vimentin*, and *α-SMA*, are highly expressed in KOA fibrotic synovium and used as markers of KOA synovial fibrosis [9, 10]. The *COL1A1* gene produces the α1 chain of type I collagen, essential for forming collagen fibrils and an integral part of the ECM [46]. Its expression is upregulated in numerous fibrotic diseases, such as idiopathic pulmonary and endometrial fibroses [47, 48]. The *CTGF* gene encodes a newly discovered multifunctional secretory protein that stimulates fibroblast proliferation and collagen deposition. It is significantly enriched in almost all fibrotic diseases, and its overexpression causes various diseases, such as glomerulosclerosis, scleroderma, liver, and pulmonary fibroses [49, 50]. The Vimentin gene encodes a type III intermediate filament protein widely distributed in the cytoskeleton with the primary role of preserving movement and integrity [51]. Its expression is also associated with many fibrotic diseases, including pulmonary fibrosis [52]. The *α-SMA* gene is now identified as a marker of myofibroblasts, known for their active proliferation and collagen secretion capabilities, contributing to fibrosis through increased ECM deposition [53]. We previously reported that significant synovial fibrosis emerges in the anterior cruciate ligament transaction (ACLT)-induced KOA rat model, as evidenced by upregulated expression of fibrosis markers TGF-β, COL1A1, and TIMP metallopeptidase inhibitor 1 (TIMP1) [54]. Therefore, interventions targeting disease-critical genes could be a vital component of therapeutic strategies against KOA synovial fibrosis.

Transforming growth factor beta (TGF-β) is a common pro-fibrotic mediator, and the key signaling pathways it activates are SMAD and the mitogen-activated protein kinase (MAPK) pathways [55]. The SMAD protein family is highly conserved, and SMAD3 is a central mediator of TGF-β signaling and is closely associated with fibrotic development in multiple organs [11]. We previously discovered that synovial macrophage pyroptosis promotes translocation of the high mobility group box 1 (HMGB1) protein from the nuclei of FLSs and binding to the renal tumor antigen (RAGE) cell surface receptor, activating the TGF-β/SMAD3 signaling pathway and attenuating synovial fibrosis [56]. The core function of TGF-β is to regulate ECM deposition and fibrosis [11] and upregulate *NUPR1* mRNA expression, which in turn enhances the transactivation potential of SMAD proteins [57]. Since TGF-β activates NUPR1 transcription through the SMAD signaling cascade [58], further investigations are needed on the role and mechanisms of NUPR1 and TGF-β/SMAD3 in KOA synovial fibrosis.

In this study, we established a model of synovial fibrosis in mice with KOA with surgical destabilization of the medial meniscus (DMM). The affected mouse joints showed obvious pathological changes of knee osteoarthritis on radiographs. Moreover, NUPR1 expression positively correlated with the pathological changes of synovial fibrosis and was upregulated in synovial tissues of mice with KOA. Next, 10-week-old male C57BL/6J mice were given an intra-articular injection of AAV expressing *NUPR1*-specific shRNA to determine whether

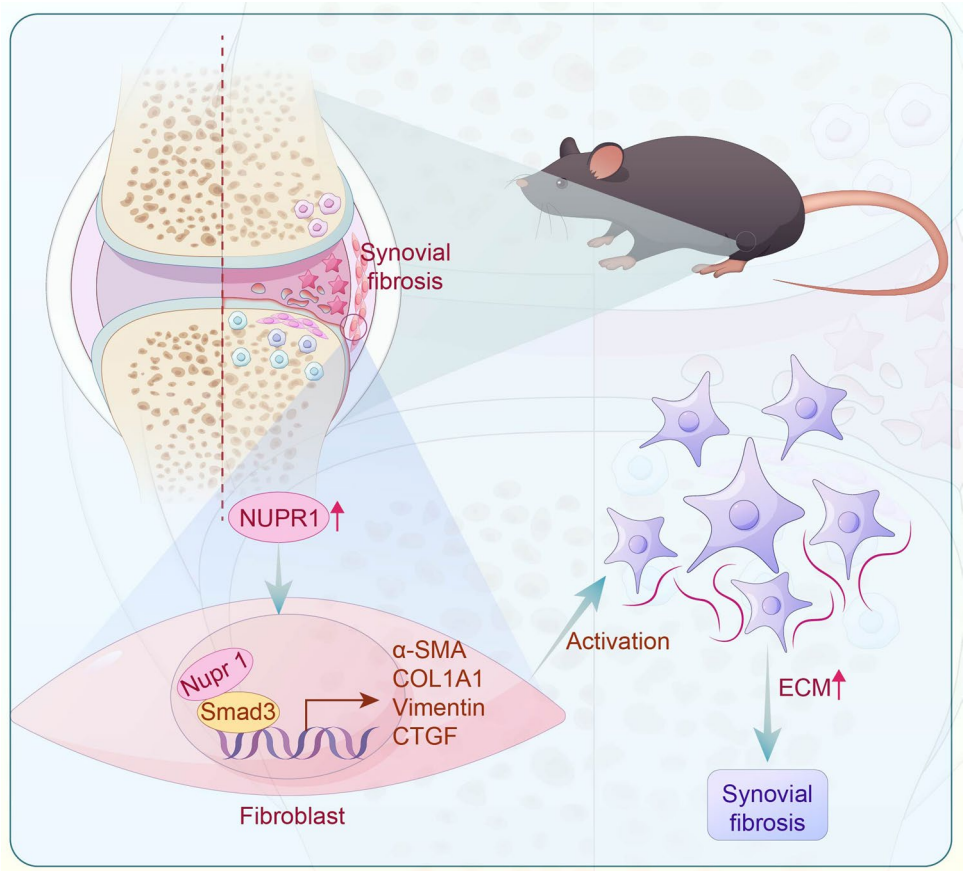


**Fig. 6** A scheme depicting the role of NUPR1 in KOA synovial fibrosis. Surgical DMM in mice induces NUPR1 expression in fibroblast-like synoviocytes. Consequently, the SMAD3 signaling pathway is activated, triggering fibroblast activation and myofibroblast transdifferentiation. Myofibroblasts, in turn, increase the extracellular matrix in synovial fibrosis

NUPR1 plays a role in synovial fibrosis. The shRNA-mediated *NUPR1* deficiency attenuated synovial fibrosis in DMM-induced synovial fibrosis. Additionally, NUPR1 deficiency inhibited synovial hyperplasia and synoviocyte proliferation. Most strikingly, silencing *NUPR1* reversed the TGF-β-triggered myofibroblast activation and mitigated TGF-β-induced synovial fibrosis by inhibiting SMAD3 phosphorylation and affecting SMAD3 nuclear localization. Ultimately, a NUPR1 inhibitor TFP alleviated synovial fibrosis by suppressing NUPR1 activity, showing pharmacologic NUPR1 inhibition may be used against synovial fibrosis (Fig. 6). However, the mechanisms by which NUPR1 influences SMAD3 phosphorylation and SMAD3 nuclear localization and additional pathological pathways driving synovial fibrosis, present unanswered questions for future research.

## Conclusions

This study found that NUPR1 expression increases in mouse synovium after surgical DMM, and NUPR1 mediates DMM-induced synovial fibrosis. Mechanistically, it shows that NUPR1 deficiency mitigates TGF-β-induced synovial fibrosis and reverses the TGF-β-induced myofibroblast activation by inhibiting SMAD3 phosphorylation and affecting SMAD3 nuclear localization. Finally, our study demonstrates that pharmacological NUPR1 inhibition is a potential strategy to treat synovial fibrosis.

**Abbreviations**

| | |
|---|---|
| KOA | Knee osteoarthritis |
| NUPR1 | Nuclear protein 1 |
| TGF-β | Transforming growth factor beta |
| SMAD3 | Smad family member 3 |
| FLSs | Fibroblast-like synoviocytes |
| ECM | Extracellular matrix |
| α-SMA | Alpha-smooth muscle |
| TFG-β | Transforming growth factor-beta 1 |
| COLLA1 | Collagen type I alpha 1 |
| CTGF | Connective tissue growth factor |
| DMM | Destabilization of medial meniscus |
| TFP | Trifluoperazine |
| AAV | Adeno-associated virus |
| HE | Hematoxylin and eosin |
| FBS | Fetal bovine serum |
| EdU | 5-Ethynyl-2′-deoxyuridine |
| IF | Immunofluorescence |
| RT-qPCR | Reverse transcription-quantitative PCR |

## Supplementary Information

The online version contains supplementary material available at https://doi.org/10.1186/s12967-024-05540-w.

Supplementary Material 1.

**Acknowledgements**
We thank the Key Laboratory for Metabolic Diseases in Chinese Medicine, Nanjing University of Chinese Medicine for the support of the experiment apparatus. We thank Bullet Edits Limited for the linguistic editing and proofreading of the manuscript. We also thank Figdraw (www.figdraw.com) for the assistance in creating Scheme (Figure 6).

**Author contributions**
TYL: Formal analysis, writing-original draft and editing; LS: Drawing figures and conceptualization; CLH: Sorting of articles and resources; DRL: Investigation and validation; YBW: Mapping and sorting tables; ZYM: Technical support; PMW: Funding acquisition and supervision; JM: Funding acquisition, Writing—review and editing; PW: Project administration and funding acquisition. All authors reviewed the manuscript. The author(s) read and approved the final manuscript.

**Funding**
The authors acknowledge financial support from the following institutions: the National Natural Science Foundation of China (Grant No. 82205143), the Excellent Young Doctor Program of Jiangsu Hospital of Chinese Medicine (Grant No. 2023QB0122), the Peak Academic Talent Project of Jiangsu Province Hospital of Chinese Medicine (Grant No. y2021rc20), the Fourth Batch of Clinical Excellence in Traditional Chinese Medicine in Jiangsu Province, the Jiangsu Provincial Medical Key Discipline (Laboratory) Cultivation Unit (Grant No. JSDW202252), the Clinical Medical Innovation Center for Knee Osteoarthritis in Jiangsu Province Hospital of Chinese Medicine (Grant No. Y2023zx05), and the Postgraduate Research & Practice Innovation Program of Jiangsu Province (Grant No. KYCX24_2216).

**Availability of data and materials**
The data supporting the findings of this study are available from the corresponding author upon reasonable request.

## Declarations

**Ethics approval and consent to participate**
All protocols and experiments were approved by the Institutional Animal Care and Use Committee of Nanjing University of Chinese Medicine (Approval No. 202302A016).

**Consent for publication**
Not applicable.

**Competing interests**
The authors declare no competing interests.

**Author details**
[1]Department of Orthopedics and Traumatology, Affiliated Hospital of Nanjing University of Chinese Medicine/Jiangsu Province Hospital of Chinese Medicine, Nanjing 210029, Jiangsu, China. [2]Key Laboratory for Metabolic Diseases in Chinese Medicine, First College of Clinical Medicine, Nanjing University of Chinese Medicine, Nanjing 210023, Jiangsu, China.

Received: 18 April 2024 Accepted: 26 July 2024
Published online: 01 August 2024

**References**

1. Allen KD, Thoma LM, Golightly YM. Epidemiology of osteoarthritis. Osteoarthr Cartil. 2022;30(2):184–95.
2. Hunter DJ, March L, Chew M. Osteoarthritis in 2020 and beyond: a Lancet Commission. Lancet. 2020;396(10264):1711–2.
3. Felson DT, Niu J, Neogi T, et al. Synovitis and the risk of knee osteoarthritis: the MOST Study. Osteoarthr Cartil. 2016;24(3):458–64.
4. Han D, Fang Y, Tan X, et al. The emerging role of fibroblast-like synoviocytes-mediated synovitis in osteoarthritis: an update. J Cell Mol Med. 2020;24:9518–32.
5. Maglaviceanu A, Wu B, Kapoor M. Fibroblast-like synoviocytes: role in synovial fibrosis associated with osteoarthritis. Wound Repair Regen. 2021;29(4):642–9.
6. Remst DF, Blaney DE, van der Kraan PM. Unravelling osteoarthritis-related synovial fibrosis: a step closer to solving joint stiffness. Rheumatology. 2015;54(11):1954–63.
7. Kasperkovitz PV, Timmer TC, Smeets TJ, et al. Fibroblast-like synoviocytes derived from patients with rheumatoid arthritis show the imprint of synovial tissue heterogeneity: evidence of a link between an increased myofibroblast-like phenotype and high-inflammation synovitis. Arthritis Rheum. 2005;52(2):430–41.
8. Steenvoorden MM, Tolboom TC, van der Pluijm G, et al. Transition of healthy to diseased synovial tissue in rheumatoid arthritis is associated with gain of mesenchymal/fibrotic characteristics. Arthritis Res Ther. 2006;8(6):R165.
9. Schuster R, Rockel JS, Kapoor M, et al. The inflammatory speech of fibroblasts. Immunol Rev. 2021;302(1):126–46.
10. Liao B, Guan M, Tan Q, et al. Low-intensity pulsed ultrasound inhibits fibroblast-like synoviocyte proliferation and reduces synovial fibrosis by regulating Wnt/beta-catenin signaling. J Orthop Translat. 2021;30:41–50.
11. Remst DF, Blaney DE, Vitters EL, et al. Osteoarthritis-related fibrosis is associated with both elevated pyridinoline cross-link formation and lysyl hydroxylase 2b expression. Osteoarthr Cartil. 2013;21(1):157–64.
12. Pineiro-Ramil M, Florez-Fernandez N, Ramil-Gomez O, et al. Antifibrotic effect of brown algae-derived fucoidans on osteoarthritic fibroblast-like synoviocytes. Carbohydr Polym. 2022;282: 119134.
13. Rim YA, Ju JH. The role of fibrosis in osteoarthritis progression. Life. 2020;11(1):3.
14. Sriwatananukulkit O, Desclaux S, Tawonsawatruk T, et al. Effectiveness of losartan on infrapatellar fat pad/synovial fibrosis and pain behavior in the monoiodoacetate-induced rat model of osteoarthritis pain. Biomed Pharmacother. 2023;158: 114121.
15. Ruiz M, Maumus M, Fonteneau G, et al. TGFbetai is involved in the chondrogenic differentiation of mesenchymal stem cells and is dysregulated in osteoarthritis. Osteoarthr Cartil. 2019;27(3):493–503.
16. Bottini A, Wu DJ, Ai R, et al. PTPN14 phosphatase and YAP promote TGFbeta signalling in rheumatoid synoviocytes. Ann Rheum Dis. 2019;78(5):600–9.
17. van Beuningen HM, Glansbeek HL, van der Kraan PM, et al. Osteoarthritis-like changes in the murine knee joint resulting from intra-articular transforming growth factor-beta injections. Osteoarthr Cartil. 2000;8(1):25–33.
18. Xie X, Gan H, Tian J, et al. Iguratimod inhibits skin fibrosis by regulating TGF-beta1/Smad signalling pathway in systemic sclerosis. Eur J Clin Invest. 2022;52(8): e13791.
19. Mallo GV, Fiedler F, Calvo EL, et al. Cloning and expression of the rat p8 cDNA, a new gene activated in pancreas during the acute phase of pancreatitis, pancreatic development, and regeneration, and which promotes cellular growth. J Biol Chem. 1997;272(51):32360–9.
20. Liu S, Costa M. The role of NUPR1 in response to stress and cancer development. Toxicol Appl Pharmacol. 2022;454: 116244.
21. Santofimia-Castano P, Huang C, Liu X, et al. NUPR1 protects against hyperPARylation-dependent cell death. Commun Biol. 2022;5(1):732.
22. Huang C, Santofimia-Castano P, Iovanna J. NUPR1: a critical regulator of the antioxidant system. Cancers. 2021;13(15):3670.
23. Borrello MT, Santofimia-Castano P, Bocchio M, et al. NUPR1 interacts with eIF2alpha and is required for resolution of the ER stress response in pancreatic tissue. FEBS J. 2021;288(13):4081–97.
24. Mu Y, Yan X, Li D, et al. NUPR1 maintains autolysosomal efflux by activating SNAP25 transcription in cancer cells. Autophagy. 2018;14(4):654–70.
25. Zhan Y, Zhang Z, Liu Y, et al. NUPR1 contributes to radiation resistance by maintaining ROS homeostasis via AhR/CYP signal axis in hepatocellular carcinoma. BMC Med. 2022;20(1):365.

26. Fan T, Wang X, Zhang S, et al. NUPR1 promotes the proliferation and metastasis of oral squamous cell carcinoma cells by activating TFE3-dependent autophagy. Signal Transduct Target Ther. 2022;7(1):130.
27. Zhang L, Gao S, Shi X, et al. NUPR1 imparts oncogenic potential in bladder cancer. Cancer Med. 2023;12(6):7149–63.
28. Yammani RR, Loeser RF. Brief report: stress-inducible nuclear protein 1 regulates matrix metalloproteinase 13 expression in human articular chondrocytes. Arthritis Rheumatol. 2014;66(5):1266–71.
29. Tan L, Register TC, Yammani RR. Age-related secline in expression of molecular chaperones induces endoplasmic reticulum stress and chondrocyte apoptosis in articular cartilage. Aging Dis. 2020;11(5):1091–102.
30. Tan L, Yammani RR. Nupr1 regulates palmitate-induced apoptosis in human articular chondrocytes. Biosci Rep. 2019;39(2): BSR20181473.
31. Zhou R, Liao J, Cai D, et al. Nupr1 mediates renal fibrosis via activating fibroblast and promoting epithelial-mesenchymal transition. FASEB J. 2021;35(3): e21381.
32. Huang C, Iovanna J, Santofimia-Castano P. Targeting fibrosis: the bridge that connects pancreatitis and pancreatic cancer. Int J Mol Sci. 2021;22(9):4970.
33. Valverde-Franco G, Hum D, Matsuo K, et al. The in vivo effect of prophylactic subchondral bone protection of osteoarthritic synovial membrane in bone-specific Ephb4-overexpressing mice. Am J Pathol. 2015;185(2):335–46.
34. Blom AB, van Lent PL, Holthuysen AE, et al. Synovial lining macrophages mediate osteophyte formation during experimental osteoarthritis. Osteoarthr Cartil. 2004;12(8):627–35.
35. Yoo SA, You S, Yoon HJ, et al. A novel pathogenic role of the ER chaperone GRP78/BiP in rheumatoid arthritis. J Exp Med. 2012;209(4):871–86.
36. Santofimia-Castano P, Xia Y, Lan W, et al. Ligand-based design identifies a potent NUPR1 inhibitor exerting anticancer activity via necroptosis. J Clin Invest. 2019;129(6):2500–13.
37. Xing R, Cheng J, Yu J, et al. Trifluoperazine reduces apoptosis and inflammatory responses in traumatic brain injury by preventing the accumulation of Aquaporin4 on the surface of brain cells. Int J Med Sci. 2023;20(6):797–809.
38. Goda AE, Elenany AM, Elsisi AE. Novel in vivo potential of trifluoperazine to ameliorate doxorubicin-induced cardiotoxicity involves suppression of NF-kappaB and apoptosis. Life Sci. 2021;283: 119849.
39. Miao Y, Chen Y, Xue F, et al. Contribution of ferroptosis and GPX4's dual functions to osteoarthritis progression. EBioMedicine. 2022;76: 103847.
40. Zhao C, Sun G, Li Y, et al. Forkhead box O3 attenuates osteoarthritis by suppressing ferroptosis through inactivation of NF-kappaB/MAPK signaling. J Orthop Translat. 2023;39:147–62.
41. Krenn V, Morawietz L, Burmester GR, et al. Synovitis score: discrimination between chronic low-grade and high-grade synovitis. Histopathology. 2006;49(4):358–64.
42. Liao T, Mei W, Zhang L, et al. L-carnitine alleviates synovitis in knee osteoarthritis by regulating lipid accumulation and mitochondrial function through the AMPK-ACC-CPT1 signaling pathway. J Orthop Surg Res. 2023;18(1):386.
43. Haubruck P, Colbath AC, Liu Y, et al. Flow cytometry analysis of immune cell subsets within the murine spleen, bone marrow, lymph nodes and synovial tissue in an osteoarthritis Model. J Vis Exp. 2020;158: e61008.
44. Liang Y, Shen L, Ni W, et al. CircGNB1 drives osteoarthritis pathogenesis by inducing oxidative stress in chondrocytes. Clin Transl Med. 2023;13(8): e1358.
45. Liao T, Ding L, Wu P, et al. Chrysin attenuates the NLRP3 inflammasome cascade to reduce synovitis and pain in KOA rats. Drug Des Devel Ther. 2020;14:3015–27.
46. Pan X, Chen X, Ren Q, et al. Single-cell transcriptomics identifies Col1a1 and Col1a2 as hub genes in obesity-induced cardiac fibrosis. Biochem Biophys Res Commun. 2022;618:30–7.
47. Li FJ, Surolia R, Li H, et al. Citrullinated vimentin mediates development and progression of lung fibrosis. Sci Transl Med. 2021;13(585): eaba2927.
48. Lin Y, Li Y, Chen P, et al. Exosome-based regimen rescues endometrial fibrosis in intrauterine adhesions via targeting clinical fibrosis biomarkers. Stem Cells Transl Med. 2023;12(3):154–68.
49. Yang Z, Li W, Song C, et al. CTGF as a multifunctional molecule for cartilage and a potential drug for osteoarthritis. Front Endocrinol. 2022;13:1040526.
50. Yanagihara T, Tsubouchi K, Gholiof M, et al. Connective-tissue growth factor contributes to TGF-beta1-induced lung fibrosis. Am J Respir Cell Mol Biol. 2022;66(3):260–70.
51. Gu C, Wang X, Long T, et al. FSTL1 interacts with VIM and promotes colorectal cancer metastasis via activating the focal adhesion signalling pathway. Cell Death Dis. 2018;9(6):654.
52. Bale S, Venkatesh P, Sunkoju M, et al. An Adaptogen: Withaferin A ameliorates in vitro and in vivo pulmonary fibrosis by modulating the interplay of fibrotic, matricelluar proteins, and cytokines. Front Pharmacol. 2018;9:248.
53. Livingston MJ, Shu S, Fan Y, et al. Tubular cells produce FGF2 via autophagy after acute kidney injury leading to fibroblast activation and renal fibrosis. Autophagy. 2023;19(1):256–77.
54. Zhang L, Zhang L, Huang Z, et al. Increased HIF-1alpha in knee osteoarthritis aggravate synovial fibrosis via fibroblast-like synoviocyte pyroptosis. Oxid Med Cell Longev. 2019;2019:6326517.
55. Guo H, Jian Z, Liu H, et al. TGF-beta1-induced EMT activation via both Smad-dependent and MAPK signaling pathways in Cu-induced pulmonary fibrosis. Toxicol Appl Pharmacol. 2021;418: 115500.
56. Wu P, Liao T, Ma Z, et al. Macrophage pyroptosis promotes synovial fibrosis through the HMGB1/TGF- beta1 axis: an in vivo and in vitro study. In Vitro Cell Dev Biol Anim. 2023;59(4):289–99.
57. Garcia-Montero AC, Vasseur S, Giono LE, et al. Transforming growth factor beta-1 enhances Smad transcriptional activity through activation of p8 gene expression. Biochem J. 2001;357(Pt 1):249–53.
58. Pommier RM, Gout J, Vincent DF, et al. The human NUPR1/P8 gene is transcriptionally activated by transforming growth factor beta via the SMAD signalling pathway. Biochem J. 2012;445(2):285–93.


## Publisher's Note